A Study of the Thermal Denaturation of Ribonuclease S by Electrospray Ionization Mass Spectrometry

David R. Goodlett*, Rachel R. Ogorzalek Loo†, Joseph A. Loo‡, Jon H. Wahl, Harold R. Udseth, and Richard D. Smith

Chemical Methods and Separations Group, Chemical Sciences Department, Pacific Northwest Laboratory, Richland, Washington, USA

The thermal stability of ribonuclease S (RNase S), an enzymatically active noncovalent complex composed of a 2166-u peptide (S-peptide) and a 11,534-u protein (S-protein), was investigated by electrospray ionization mass spectrometry (ESI-MS) and capillary electrophoresis ESI-MS (CE-ESI-MS). The intensities of peaks corresponding to the RNase S complex were inversely related to both the applied nozzle–skimmer (or capillary–skimmer) voltage bias in the atmosphere–vacuum interface and the temperature of the RNase S solution. By using a heated metal capillary–skimmer interface and a room temperature solution of RNase S, the intensities of RNase S molecular ion peaks were observed to decrease with increasing metal capillary temperature. Mass spectrometric studies with both the nozzle–skimmer and capillary–skimmer interface designs allowed determination of phenomenological enthalpies for dissociation of the RNase S complex in both solution and for the electrosprayed microdroplet–gas phase species. Intact RNase S complex could also be detected with CE-ESI-MS separations by using a 10-mM ammonium bicarbonate (pH 7.9) solution as the electrophoretic buffer. These studies provide new insights into the stability of multiply charged noncovalent complexes in the gas phase and the mass spectrometric conditions required for such studies, and suggest that information regarding solution properties can be obtained by ESI-MS. *(J Am Soc Mass Spectrom 1994, 5, 614–622)*

Increasingly, electrospray ionization mass spectrometry (ESI-MS) [1–6] is being used to examine the noncovalent interactions between biological macromolecular species such as ligands and receptors [7–10], subunits in protein complexes [11, 12], and oligonucleotides [13–15]. To use ESI-MS for studying specific interactions between noncovalently associated macromolecules that occur in solution, care must be exercised to ensure that transfer to the gas phase minimizes dissociation of the complex [16, 17]. A few studies have reported the effects on resultant mass spectra due to thermally denaturing biomolecules in solution prior to ESI-MS analysis [18–20], and such studies also suggest that the gas phase complexes do in fact arise from specific associations in solution. Thermal denaturation in solution has allowed detection and molecular weight measurements for glycoproteins by ESI-MS in cases where mass spectra could not be obtained with corresponding room temperature solutions [18, 19]. Also, the enthalpy of thermal denaturation ($\Delta H_{denaturation}$) for cytochrome *c* was obtained from examination of changes in the charge state distribution at different solution temperatures [20]. These results suggest broad new applications of mass spectrometry for the study of solution associations, as well as possible applications for screening compounds that have specific interactions, perhaps even from large collections of similar compounds (e.g., polypeptide libraries).

In this article we describe the application of the protein ribonuclease S (RNase S) as a model system for investigation of processes relevant to the detection of noncovalent complexes by ESI-MS. We have explored denaturation of the complex in the ESI-MS interface to examine its role in maintaining or denaturing noncovalent interactions in the microdroplet–gas-phase environment. In addition, we report the use of capillary electrophoresis ESI-MS (CE-ESI-MS) to investigate the S-protein–S-peptide solution interaction under acidic

Address reprint requests to Dr. Richard D. Smith, Chemical Methods and Separations Group, Chemical Sciences Department, Battelle, Pacific Northwest Laboratory, Box 999, P8-19, Richland, WA 99352.
* Current address: Immunobiology Research Institute, Route 22 East, P.O. Box 999, Annandale, NJ 08801-0999.
† Current address: Protein and Carbohydrate Structure Facility, University of Michigan, 2552 MSRB II, Ann Arbor, MI 48109.
‡ Current address: Parke-Davis Pharmaceutical Research Division, 2800 Plymouth Road, Ann Arbor, MI 48105.

1044-0305/94/$7.00

Received September 28, 1993
Revised February 17, 1994
Accepted February 17, 1994

and mildly alkaline buffer conditions, conditions under which the complex is unstable and stable in solution, respectively. Because many noncovalently associated macromolecular complexes are quite thermally labile [21], we investigated thermal denaturation in both the solution and in the microdroplet–gas phases to examine the specificity of interaction between the two RNase S complex components, that is, the S-peptide and the S-protein. Our results indicate that one must exercise caution in drawing conclusions about solution phase interactions based on ESI-MS data, an issue recently discussed at length by Smith and Light-Wahl [5]. However, if appropriate care is taken to ensure that complex stability results are not skewed by the mass spectrometry detection methods [5], ESI-MS constitutes a useful approach for examining the stability of, and the determination of binding constants between, macromolecular subunits in thermally labile noncovalent complexes.

Experimental

Capillary Electrophoresis

The CE instrumentation used in this study has been described in detail previously [23]. Capillary electrophoresis was conducted using fused-silica capillaries with dimensions 50 μm i.d. × 185 μm o.d. (Polymicro Technologies, Phoenix, AZ). For CE with acidic buffers, the surface of the fused-silica capillaries was modified with aminopropylsilane [22]. Electrophoretic separations were carried out in 10-mM acetic acid, pH 3.4, or 10-mM ammonium bicarbonate, pH 7.9, by using 100-cm-long capillaries and an electric field strength of 300 V/cm. The protein solution was injected by using the electrokinetic method at 300 V/cm for 10 s.

Mass Spectrometry

The ESI source used for both direct infusion and "on-line" CE-MS, and the quadrupole mass spectrometer have been described previously [24] and were used without modification. The quadrupole mass spectrometer interface used in most studies consists of a nozzle–skimmer atmospheric pressure inlet, followed by an integral cryopumping arrangement that provides very high pumping speeds ($> 10^5$ L/s). Operating pressures in the analysis quadrupole, which is separated from the radiofrequency-only quadrupole located in a differentially pumped intermediate chamber, were typically $\sim 10^{-7}$ torr. The ion sampling orifice had a 1.0-mm-diameter opening and was generally maintained at room temperature. Alternatively, in separate experiments the nozzle–skimmer interface was replaced with a resistively heated, "Y"-shaped metal capillary–skimmer inlet that incorporated two 6-in.-long inlet arms, with one arm capped and the other open to the atmospheric-pressure ESI source [25, 26]. This Y-tube was fabricated from 0.0625-in.-o.d., 0.040- or 0.020-in. i.d. stainless steel tubing. The capillary or ion sampling orifice potential and quadrupole offset voltages were optimized (for preservation of noncovalent interactions) relative to the skimmer, which was maintained at ground potential. An unheated countercurrent nitrogen stream was used to assist desolvation with the nozzle–skimmer interface, whereas in some experiments with the capillary–skimmer interface (noted) a transverse stream of nitrogen was employed. A coaxial stream of sulfur hexafluoride (50 mL/min) around the infusion or CE capillary was used to suppress electrical discharges in the ESI source. The voltage applied to the ESI source (emitter) was optimized between 4.5 and 6.5 kV, and the distance from the ESI emitter to the nozzle or Y-tube orifice was ~ 1 cm. Distilled deionized water (3.3 μL/min) was used as the sheath liquid to eliminate possible denaturation of RNase S by organic sheath liquids. The mass spectrometer was generally scanned from m/z 500 to 2000 with a dwell time of 1 ms/u and operated at a nominal resolution of 300–400.

For liquid-phase thermal denaturation studies, a 60-cm-length region of the total 80-cm length of 50-μm-i.d. × 185-μm-o.d. fused-silica capillary was thermally regulated by using heating tape, leaving unheated capillary segments of about 8 cm at the ESI source and 12 cm at the syringe. Temperature was measured by a thermocouple placed inside the heating tape. "On-line" thermal denaturation [18–20] was conducted by filling the capillary with the sample solution, incubating for 10 min at a given temperature, and then directly infusing the sample at 0.5 μL/min with a syringe pump (Harvard Apparatus, South Natick, MA) into the ESI source. As an alternative to on-line incubation, room-temperature (28 ± 1 °C) solutions of RNase S were also directly infused through the heated capillary (at 0.5 μL/min). Transport time through the heated infusion capillary during infusion was about 2 min. Direct infusion of RNase S at temperatures below room temperature was accomplished by immersing the fused-silica capillary in a water bath maintained at 4 °C. For applications using the metal capillary–skimmer interface, solutions of RNase S at room temperature were electrosprayed into the capillary inlet, which was heated over a range of 50 to 200 °C. Metal capillary temperature was measured on the outside of the Y-tube wall by a chromel–alumel thermocouple.

Sample Preparation and Handling

Bovine pancreatic ribonuclease S (RNase S; lot number 61H7191) was purchased from Sigma Chemical Company (St. Louis, MO) and used without further purification. All water for sample dissolution and the liquid

coaxial sheath of the ESI source was distilled and deionized. Solutions of RNase S were prepared in distilled deionized water at a 73-μM concentration, then stored at −20 °C. Prior to use, solutions of RNase S were thawed at 4 °C.

Results and Discussion

Ribonuclease S Structure and Activity

Ribonuclease S (M_r = 13,700) is an enzymatically active biochemically well characterized noncovalent complex composed of a 2166-u peptide (S-peptide, residues 1–21) and a 11,534-u protein (S-protein, residues 22–124), which cleaves phosphodiester bonds within ribonucleic acids with a preference for pyrimidines [27]. Ribonuclease S is produced by limited proteolytic cleavage of ribonuclease A (RNase A) at amide bond 21 by subtilisin [27]. Lack of substrate (RNase S) specificity at the site of cleavage also results in some cleavage between serine residues 20 and 21, producing a second S-peptide (residues 1–20) and S-protein (residues 21–124); both sets are present in the samples used in these studies. The specific activity of RNase A is retained by RNase S, indicating that important structural features (i.e., orientation of S-peptide His-12 and S-protein His-119) are maintained because both residues are necessary for its catalytic activity. Ribonuclease S is known to lose enzymatic activity at a lower temperature than RNase A, presumably due to physical dissociation of S-peptide from S-protein [28]. Dissociation of RNase S also can be induced by a decrease in pH, which results in protonation of S-peptide side chain residues Lys-7, Arg-10, and His-12 [29], followed by the loss of the α-helical S-peptide structure. This loss of S-peptide α-helical structure allows physical dissociation of S-peptide from S-protein by a one-step process [29]. Previously published ESI mass spectra of RNase S in dilute solution of acetic acid [30, 31] showed peaks corresponding to the S-protein and S-peptide, but not intact RNase S, consistent with the expected acid-induced dissociation of RNase S in solution [32]. However, these early ESI-MS studies also did not employ the gentle interface conditions that more recently have been demonstrated to be necessary for preservation of such noncovalent complexes, as we described in a short communication for RNase S [32].

Solution conditions conducive to observation of RNase S ions were selected based on previous work that found RNase S completely dissociated in acidic solutions [21], but stable at or near pH 7.0. Ribonuclease S prepared in 5% acetic acid produced mass spectra devoid of peaks for intact RNase S, and contained only peaks due to the S-peptide and S-protein [32]. RNase S dissolved in distilled deionized water with an unbuffered pH of ~ 6.0 preserves the complex in solution [32], consistent with the capillary electrophoresis results presented (see later discussion). The following discussion of mass spectrometric conditions necessary for observation of RNase S ions assumes the use of distilled deionized water as a solvent for RNase S.

Use of a Nozzle–Skimmer ESI Interface to Observe Ribonuclease S

Observation of intact RNase S complex by ESI-MS requires a compromise between the conflicting conditions required to obtain efficient desolvation and to minimize complex dissociation so as to provide useful mass spectrometric signal intensities for the complex. The interface conditions utilized for observation of the noncovalent complex between S-peptide and S-protein involved a combination of the following parameters: (1) a low nozzle–skimmer bias (ΔNS), (2) a coaxial sheath of distilled deionized water, and (3) use of an unheated countercurrent nitrogen gas flow. The low ΔNS was the single most important factor for observation of the noncovalent complex. Use of a methanol coaxial sheath, rather than deionized water, resulted in a large reduction in RNase S intensity, as did the application of a heated countercurrent gas.

Figure 1 illustrates the dramatic effect of collisional activation in the interface, by variation of ΔNS voltage, on the ESI-MS spectrum. When an aqueous solution of RNase S is electrosprayed at ΔNS = 300 V (Figure 1a), no RNase S peaks are evident. The mass spectrum of the same solution electrosprayed at ΔNS = 100 V (Figure 1b) is dominated by peaks arising from intact RNase S. Qualitatively, the changes observed in the spectra at higher ΔNS are comparable to those obtained by using denaturing solvent conditions. The broader peaks observed for RNase S at ΔNS = 100 V (Figure 1b) reflect the poorer desolvation and/or greater extent of residual phosphate (or sulfate) adduction and possibly other contributions at gentler interface conditions (i.e., lower ΔNS) [32]. At ΔNS = 300 V the spectrum also shows doubly charged S-peptide (1–20) and (1–21) species, which differ by one serine residue, and the corresponding more highly charged S-protein (21–124) and (22–124) species [28]. Additional S-protein-derived peaks due to phosphate (or sulfate) adducts [32, 33] are also observed. In the case of RNase S, phosphate can bind to the active site, which stabilizes the complex [28]. The phosphate adducts are most likely due to contaminants from buffers used during purification [27]. Under the mass spectrometric conditions used in this study, ions for S-protein (21–124) cannot be unambiguously resolved from S-protein (22–124) peaks that possess a single 98-u phosphate adduct. However, separate *low resolution* tandem mass spectrometry experiments on the peaks with a TAGA 6000E triple quadrupole instrument (Sciex, Thornhill, Ontario, Canada) were able to separate the different species (data not shown) due to the putative multiply charged S-protein species and adduct ions. For example, by using the more highly

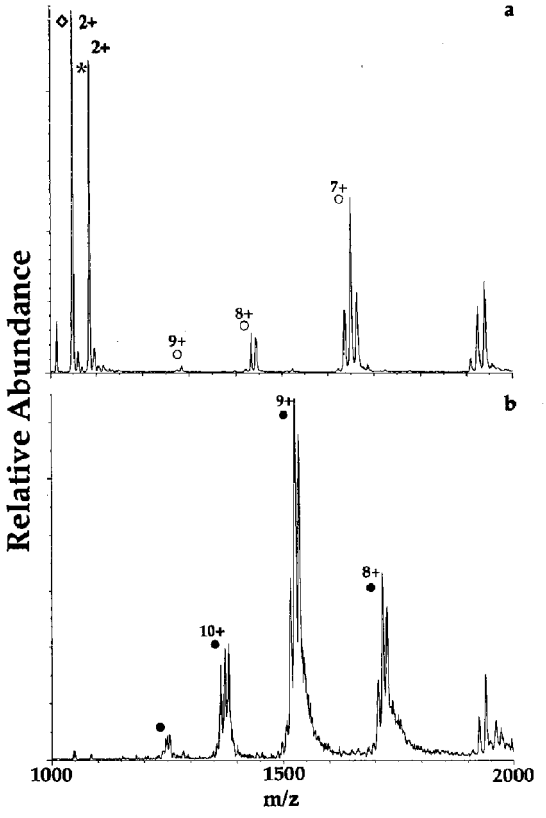

Figure 1. ESI-MS of a 73-μM solution of RNase S at room temperature with a nozzle–skimmer interface voltage bias (ΔNS) of (a) 300 V (high) and (b) 100 V (low). Peaks due to the S-protein (○) and RNase S (●) are indicated. The major peaks for the 7+ charge state are attributed to S protein (22–124), S-protein (22–124) + H_3PO_4 or S-protein (21–124), and S-protein (21–124) + H_3PO_4 or S-protein (22–124) + $2H_3PO_4$ [32]. The ions labeled ◇ and * are the doubly protonated ions for the S-peptides (1–20) and (1–21), respectively.

phosphate-adducted sample examined previously [32] (and more gentle interface conditions; see later discussion of Figure 5), tandem mass spectrometry (MS/MS) of the ion at m/z 1304 produce ions at both m/z 1293 and 1282. The m/z 1304 species is assigned as the 9+ molecular ion for (21–124) with two phosphate–sulfate adducts. Dissociation of this species yields (21–124) with one adduct (m/z 1293) and the (21–124) species with no adducts (m/z 1282). MS/MS of m/z 1293 yields m/z 1282, but also m/z 1272, which is most likely the (22–124) species. Thus, a small fraction of the peaks at m/z 1293 and 1282 can be attributed to adduct ions for the (22–124) species.

Figure 2 shows the relationship between ΔNS and the sum of ion intensities for all charge states observed for RNase S divided by the sum of ion intensities for all observed charge states from S-protein ion intensity. Each datum point represents the average of 10 scans obtained during direct infusion of a room-temperature

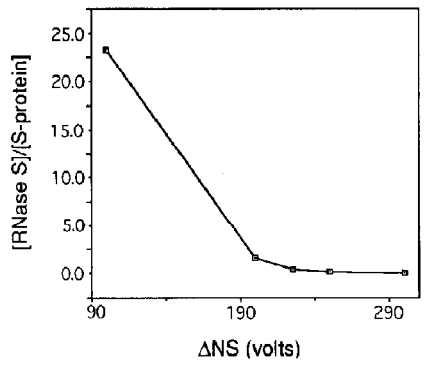

Figure 2. The effect of increasing ΔNS on RNase S intensity. The sum of peak intensities for all charge states observed for RNase S was divided by the sum for all S-protein charge states and plotted versus ΔNS. A 73-μM solution of RNase S at 27–29 °C was used.

RNase S solution using the "soft" interface conditions described above. Elevating the ΔNS above 200 V dramatically decreases the intensity of RNase S ion abundance due to collisional dissociation processes.

CE-ESI-MS of Ribonuclease S with the Nozzle–Skimmer Interface

When an aqueous solution of RNase S was examined at room temperature with CE-ESI-MS by using a 10-mM acetic acid (pH 3.4) buffer and ΔNS = 100 V, the separation yielded two peaks (insert of Figure 3a), corresponding to S-peptide and S-protein, due to dissociation of the RNase S early in the electrophoretic separation. The total ion electropherogram (TIE) was quite noisy, due largely to the nonoptimal ESI-MS interface conditions necessary for detection of any noncovalent complex. The mass spectrum for the first peak showed only ions for the S-peptide (data not shown), whereas the mass spectrum for the second peak showed only ions for the S-protein (Figure 3a). No other scans from the TIE showed peaks due to the S-peptide, S-protein, or RNase S. A similar CE-MS separation conducted in a 10-mM ammonium bicarbonate buffer (pH 7.9) produced a TIE with only one broad peak (insert of Figure 3b) that showed peaks due to the intact RNase S complex. A second CE-MS experiment conducted by using 10-mM ammonium bicarbonate at high ΔNS (250 V) also resulted in only one broad peak on the TIE, and yielded mass spectra corresponding to the S-peptide and S-protein. The contributions of S-peptide and S-protein ions to the mass spectrum (Figure 3b) at low ΔNS (100 V) do not rule out the possibility that some small amount of dissociation of RNase S occurred during electrophoresis, but more likely reflect a small contribution from dissociation in the interface. However, it is also possible that loss of native α-helical structure for some fraction of the S-peptide population during electrophoresis could result

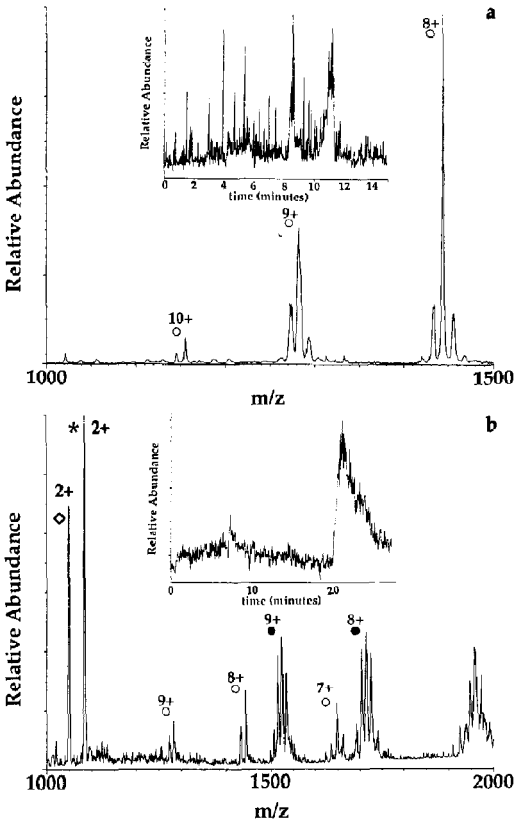

Figure 3. Positive-ion CE-MS of a 73-μM solution of RNase S in either **(a)** 10-mM acetic acid, pH 3.4, in an aminopropyl-derivatized fused-silica capillary at −30 kV and **(b)** 10-mM ammonium bicarbonate, pH 7.9, in an underivatized fused-silica capillary at +30 kV. Mass spectra correspond to **(a)** the S-protein and **(b)** RNase S. Peaks in **(b)** also arise because of the S-protein (○) ions, S-peptide (1–21) (*), and S-peptide (1–20) (◇) due to RNase S dissociation in the interface.

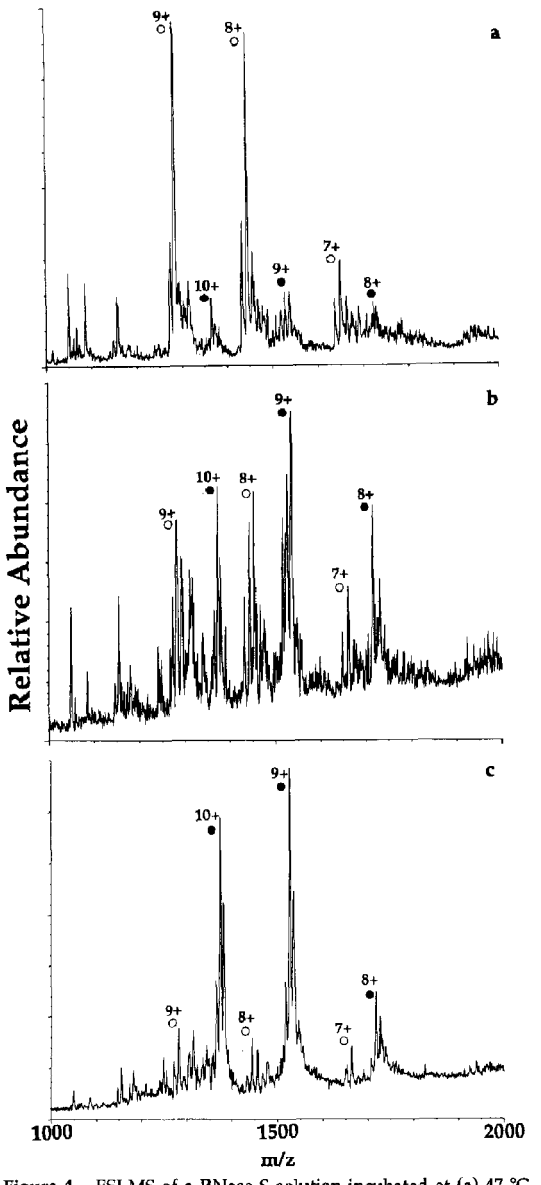

Figure 4. ESI-MS of a RNase S solution incubated at **(a)** 47 °C, **(b)** 41 °C, and **(c)** 30 °C for 10 min prior to analysis with ΔNS = 150 V. Peaks due to the S-protein (○) and RNase S (●) are indicated.

in some portion of the RNase S entering the electrospray in a conformation that might be less stable to dissociation than native RNase S, even at low ΔNS. These less-stable RNase S complexes (RNase S′) would be less likely to survive the electrospray process than the more compact structure of native RNase S, and give rise to the S-protein and S-peptide peaks in Figure 3b. However, the above results show that at pH 7.9 most of the RNase S complex remains intact during electrophoresis and can be successfully analyzed by CE-ESI-MS under appropriate interface conditions.

Thermal Denaturation of Ribonuclease S in the Liquid Phase

Incubation of RNase S at 60 °C followed by direct infusion through a fused-silica capillary (also maintained at 60 °C) produced mass spectra at a low ΔNS (100 V) that showed peaks due to S-peptide and S-protein, but not RNase S. Mass spectra obtained at a constant ΔNS = 150 V after incubation and direct infusion of RNase S at 30, 41, and 47 °C are shown in Figure 4 and demonstrate an inverse relationship between the RNase S solution temperature and the RNase S molecular ion intensities. By thawing a RNase S solution at 4 °C and directly infusing the cold RNase S solution through a fused-silica capillary submerged in an ice and water bath, it was possible to increase the proportion of RNase S ions observed beyond that ob-

served by infusion at room temperature (data not shown). However, small S-peptide peaks still contribute to these "low temperature" mass spectra, suggesting that some fraction of the RNase S complex is still dissociated in the ESI interface. Results obtained at the lower ΔNS (< 50 V), where the relative intensities of S-peptide peaks are smaller (data not shown), are consistent with this concept. However, the greater instability and lower signal intensities of the ESI spectra at low ΔNS precluded thermodynamic studies in the present work.

Use of the Capillary–Skimmer Interface to Observe Ribonuclease S

When a heated metal capillary–skimmer interface was used in place of a nozzle–skimmer interface, the RNase S complex was generally more difficult to observe. Note that this is not a general observation: we have observed that some noncovalent complexes are more readily detected by using the heated metal capillary inlet [14]. However, the application of a room-temperature stream of nitrogen, transverse to the spray direction, allowed usable mass spectra for the complex to be obtained at lower inlet temperatures. In a comparison of the 1.0- and 0.5-mm-i.d. inlet capillaries, it was observed that the larger capillary i.d. generally required higher capillary temperatures and/or higher capillary–skimmer biases (ΔCS) to achieve the same degree of desolvation. This observation most likely reflects both the greater gas volume to be heated and the greater solvent cooling in the expansion with the larger capillary diameter under a given set of experimental conditions (i.e., ΔCS, capillary–skimmer distance, and effective pumping rates). The average temperature difference between the capillary wall and the gas also is expected to be greater with the larger i.d. capillary inlets. Consistent with this hypothesis, at a given capillary temperature, molecular ion peaks from the 1.0-mm-i.d. inlet capillary are broader than those peaks obtained by using the 0.5-mm-i.d. capillary. In essence, as the capillary diameter increases, the effective capillary temperature is reduced and the behavior becomes more similar to that of the nozzle–skimmer interface.

Thermal Denaturation of Ribonuclease S in the Microdroplet–Gas Phase

To compare the results obtained by heating the solution in the fused-silica capillary with the results of collisional activation in the nozzle–skimmer interface, experiments were carried out by electrospraying a solution of RNase S at room temperature into a heated metal capillary–skimmer interface. While maintaining a constant ΔCS, the temperature of the exterior of the metal capillary was varied from 88 to 171 °C. At a metal capillary temperature of 110 °C, peaks due to

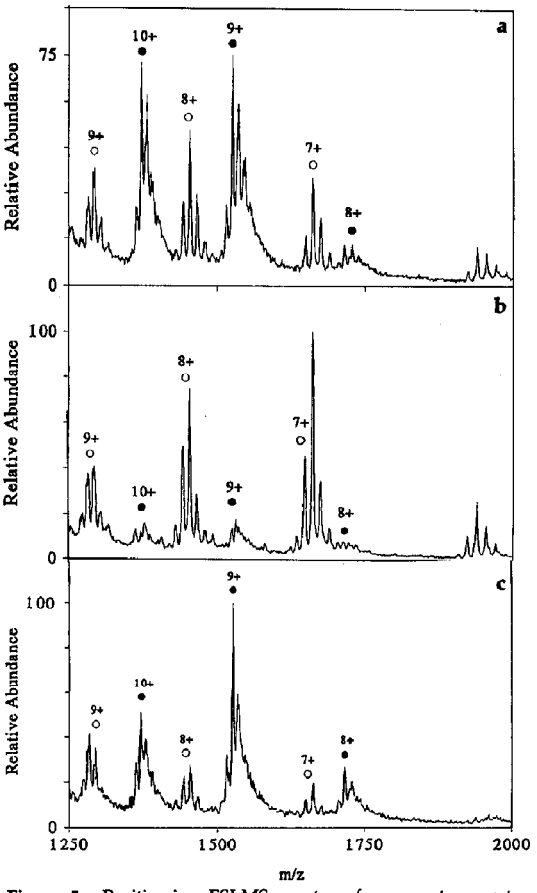

Figure 5. Positive-ion ESI-MS spectra of a room-temperature 73-μM solution of RNase S with a metal capillary interface at a temperature of 110 °C (top) and 171 °C (middle), with ΔCS = 0 V in both cases, and with a metal capillary interface at a temperature of 88 °C and ΔCS = 200 V (bottom). Peaks due to the S-protein (○) and RNase S (●) are indicated.

intact RNase S were observed along with peaks due to S-protein (Figure 5a). At the higher capillary temperature of 171 °C (Figure 5b) nearly all contributions due to RNase S are absent. The lability of the RNase S complex ions at these temperatures is likely to result from several factors. First, RNase S enters the capillary dispersed in approximately micrometer size droplets produced by the electrospray process. Cooling of the droplets due to evaporation and the thermal lag in *gas* temperature (compared to the metal capillary *wall* temperature) assures that the effective temperature of RNase S is considerably lower than the capillary walls during most of the transit through the capillary. Second, residence time in the capillary is limited to only a few milliseconds so that, compared to solution studies, much higher dissociation rates are needed to induce dissociation in the droplet or gas phase during the residence time in the capillary. The observed effects of capillary wall temperature and ΔCS on preservation of

RNase S were comparable; similar spectra could also be obtained by increasing one factor while lowering the other. Figure 5a and b illustrate the effect of capillary temperature at a constant $\Delta CS = 0$ V. Figure 5c shows that the RNase S complex also can be observed with $\Delta CS = 200$ V with an exterior capillary temperature of 88 °C. At this same $\Delta CS = 200$ V, peaks for RNase S would be absent at an inlet temperature of 110 °C, which suggests that the more highly solvated complexes emerging from the capillary are stable even at relatively high ΔCS because they can dissipate collisional energy through solvent evaporation. Thus, preservation of the association between S-peptide and S-protein for mass spectrometric detection requires a balance between preserving the noncovalent interactions and heating to achieve effective desolvation, and it appears that the details of the time versus temperature profile through the ESI interface are important for more labile complexes.

Interpretation of Thermal Denaturation Data—Liquid Phase

To study the solution interaction between the S-peptide and S-protein at various solution temperatures for determining solution thermodynamic properties (e.g., enthalpy of dissociation), it is important to understand (i.e., minimize) possible confounding contributions that arise from dissociation of the complex in the mass spectrometric interface. Results for RNase S incubated at various solution temperatures suggest the possibility that solution temperature may affect the fraction of the remaining RNase S that dissociates in the interface. A possible explanation for such behavior can be suggested. Solvent evaporation can be expected to proceed more quickly in the ESI interface for the higher solution temperatures, allowing the microdroplets to be smaller and a higher effective temperature to be obtained in the interface. If the microdroplets exiting the inlet are "dryer," then fewer solvent molecules are available to dissipate collisional energy by evaporation. If such an effect were significant, the result would be a greater overall extent of dissociation in the interface. Alternatively, a similar enhancement in dissociation also could arise from structural modification of the RNase S to a more labile form.

The effect of ΔNS bias on dissociation is illustrated by the van't Hoff plots shown in Figure 6, obtained by using relative ion intensities for the S-protein and RNase S species collected at three different solution temperatures and two different ΔNS values (150 and 200 V). The van't Hoff plots were produced by plotting log([S-protein]^2/[RNase S]) versus the reciprocal of the solution temperature. (The S-peptide peak intensities were not used in the van't Hoff plot because the large difference in molecular weights between S-peptide and RNase-S [13] could lead to dramatically different detection efficiencies, whereas the S-protein detector efficiency is expected to be closer to that of RNase.) As

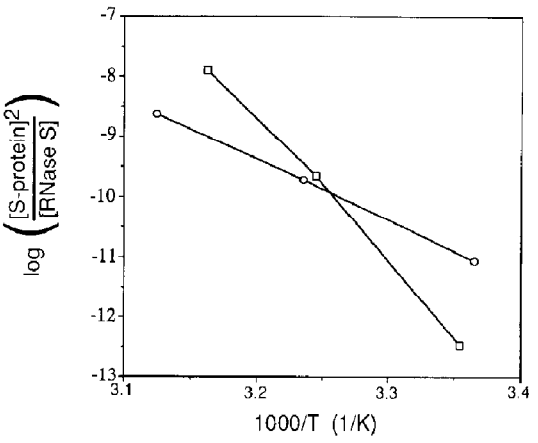

Figure 6. Plot of log([S-protein]^2/[RNase S]) versus sample temperature at $\Delta NS = 150$ V (□) or 200 V (○). Each datum point represents the sum of 10 scans at each temperature. The $\Delta H_{dissociation}$ shows a dependence on ESI interface conditions, indicating that interface activation needs to be minimized and interface contributions need to be considered in such studies.

seen in Figure 6, at $\Delta NS = 200$ V (○) a $\Delta H_{dissociation}$ of +20 kcal/mol was determined, whereas at $\Delta NS = 150$ V (□) a $\Delta H_{dissociation}$ of +48 kcal/mol was obtained. Literature values for $\Delta H_{dissociation}$ under conditions identical to those necessary for mass spectrometry (i.e., low ionic strength) are not available. However, the $\Delta H_{dissociation}$ values from our ESI-MS data are of similar magnitude to those values found in the literature, which range from 29 to 40 kcal/mol [29, 34]. Solution conditions, such as ionic strength and pH are important parameters that can affect the thermodynamic values measured by calorimetry, but ESI-MS is currently more effectively accomplished with low ionic strength solutions and volatile buffers.

The present data suggest that useful thermodynamic values are best obtained under the gentlest possible interface conditions. The effect of interface conditions might be expected to cause the enthalpy to be *underestimated.* It is obvious from the van't Hoff plots that the ΔNS selected for such studies should be minimized.

Interpretation of Thermal Denaturation Data—Microdroplet–Gas Phase

To compare the nozzle–skimmer interface and capillary–skimmer interface designs, a van't Hoff analysis also was made of data from the thermal dissociation of RNase S in a heated metal capillary. A phenomenological $\Delta H_{dissociation}$ of + 21 kcal/mol was calculated for data obtained at $\Delta CS = 0$ V. However, measurement of an irreversible dissociation event in the heated metal capillary is probably more accurately described as an energy of activation rather than an enthalpy of dissociation. Because the dissociation being measured occurs

in a continuously changing environment that spans the reversible microdroplet phase and the irreversible gas phase, cautious comparison with solution measurements is clearly warranted.

From a practical point of view there may appear to be little difference between activation of the molecule during transport through the metal capillary or after exiting the capillary (i.e., in the capillary–skimmer region). However, there are fundamental differences between heating in these two regimes. For applications that do not employ a countercurrent or transverse stream of drying gas, the species of interest almost certainly enters the capillary inlet in microdroplets. Thus, heating in the early part of the capillary inlet most likely affects solution behavior, whereas collisional heating in the interface or heating in the latter part of the capillary should reflect gas-phase behavior. Solution conditions in the highly charged droplets can be expected to change as evaporation proceeds. Gas-phase processes involving like-charge polarity species, such as dissociation of the S-peptide and S-protein, are probably irreversible and measurements are more likely to yield activation energies. From an alternate point of view, conditions that reflect reversible solution interactions should suggest the magnitudes of equilibrium constants, whereas conditions that reflect irreversible gas-phase interactions are more likely to indicate the *avidity* of binding, an equally important parameter.

Conclusions

The presented results show that, with care, ESI-MS can provide insights into macromolecular associations in solution. An inverse relationship has been observed between the temperature of an RNase S solution and the stability of the RNase S complex in the gas phase. This trend is in agreement with previously reported thermal denaturation studies where the RNase S enzymatic activity was lost at higher temperatures because of physical separation of active sites [32].

Ions for the intact RNase S complex can be observed with both the heated metal capillary–skimmer and nozzle–skimmer interfaces. A room temperature solution of RNase S showed an inverse relationship between RNase S ion abundance and metal capillary temperature. Observation of thermally labile RNase S at high metal capillary temperatures is possible due to the limited residence time of the complex in the metal capillary and an effective gas temperature in the capillary that is lower than the capillary wall temperature.

Until the ESI-MS interfacial contributions to complex dissociation are better understood, the use of on-line thermal denaturation studies as described in this work to determine thermodynamic properties of noncovalently associated macromolecular complexes must be approached with caution. Smith and Light-Wahl [5] have advanced criteria based on several types of mass spectrometric data that can provide various levels of confidence for possible specific associations. Although the experimental enthalpies derived from this work are of lower precision than calorimetric results, such studies may be qualitatively useful for rapidly characterizing small quantities of novel complexes. Better control of ESI interface conditions also should allow much greater precision for such measurements. On-line thermodynamic investigations of macromolecular complexes using CE-ESI-MS should be feasible on femtomole-level quantities of a sample. It should also be possible to conduct comparative studies from mixtures of similar species. In cases where a limited quantity of a novel biological complex is available, obtaining thermodynamic measurements by thermal denaturation during CE-ESI-MS would be a valuable aid in the initial characterization. Moreover, the CE separation offers an alternate approach for evaluating dissociation constants independent of the ESI-MS interface.

Acknowledgment

This research was supported by the U.S. Department of Energy under contract DE-AC06-76RLO 1830. Pacific Northwest Laboratory is operated by Battelle Memorial Institute.

References

1. Wong, S. F.; Meng, C. K.; Fenn, J. B. *J. Phys. Chem.* **1988**, *92*, 546.
2. Fenn, J. B.; Mann, M.; Meng, C. K.; Wong, S. F.; Whitehouse, C. M. *Science* **1989**, *246*, 64.
3. Bruins, A. P.; Covey, T. R.; Henion, J. D. *Anal. Chem.* **1987**, *59*, 2642.
4. Covey, T. R.; Boner, R. F.; Cushion, B. I.; Henion, J. D. *Rapid Commun. Mass Spectrom.* **1988**, *2*, 249.
5. Smith, R. D.; Light-Wahl, K. J. *Biol. Mass Spectrom.* **1993**, *22*, 493.
6. Smith, R. D.; Loo, J. A.; Edmonds, C. G.; Barinaga, C. J.; Udseth, H. R. *Anal. Chem.* **1990**, *62*, 882.
7. Ganem, B.; Li, Y.-T.; Henion, J. D. *J. Am. Chem. Soc.* **1991**, *113*, 6294.
8. Ganem, B.; Li, Y.-T.; Henion, J. D. *J. Am. Chem. Soc.* **1991**, *113*, 7818.
9. Ganguly, A. T.; Pramanik, B. N.; Tsarbopoulos, A.; Covey, T. R.; Huang, E.; Fuhrman, S. A. *J. Am. Chem. Soc.* **1992**, *114*, 6559.
10. Lumb, K. J.; Aplin, R. T.; Radford, S. E.; Archer, D. B.; Jeenes, D. J.; Lambert, N.; Mackenzie, D. A.; Dobson, C. M.; Lowe, G. *FEBS* **1992**, *296*, 153.
11. Katta, V.; Chait, B. T. *J. Am. Chem. Soc.* **1991**, *113*, 8534.
12. Baca, M.; Kent, S. B. H. *J. Am. Chem. Soc.* **1992**, *114*, 3992.
13. Goodlett, D. R.; Camp, D. G., II; Hardin, C. C.; Corregan, M.; Smith, R. D. *Biol. Mass Spectrom.* **1993**, *22*, 81.
14. Light-Wahl, K. J.; Springer, D. L.; Winger, B. E.; Edmonds, C. G.; Camp, D. G., II; Thrall, B. D.; Smith, R. D. *J. Am. Chem. Soc.* **1993**, *115*, 803.
15. Ganem, B.; Li, Y.-T.; Henion, J. D. *Tetrahedron Lett.* **1993**, *34*, 1445.
16. Smith, R. D.; Light-Wahl, K. J.; Winger, B. E.; Loo, J. A. *Org. Mass Spectrom.* **1992**, *27*, 811.
17. Meng, C. K.; Fenn, J. B. *Org. Mass Spectrom.* **1991**, *26*, 542.
18. Mirza, U. A.; Cohen, S. L.; Chait, B. T. *Anal. Chem.* **1993**, *65*, 1.

19. Allen, M. H.; Vestal, M. L. *J. Am. Soc. Mass Spectrom.* **1992**, *3*, 18.
20. LeBlanc, J. C. Y.; Beuchemin, D.; Siu, K. W. M.; Guevremont, R.; Berman, S. S. *Org. Mass Spectrom.* **1991**, *26*, 831.
21. Privalov, P. L. In *Advances in Protein Chemistry*, Vol. 33; Anfinsen, C. B.; Edsall, J. T.; Richards, F. M., Eds.; Academic: New York, 1979; p 167.
22. Bruin, G. L. M.; Huisden, R.; Kraak, J. C.; Poppe, H. *J. Chromatogr.* **1989**, *480*, 339.
23. Smith, R. D.; Udseth, H. R.; Barinaga, C. J.; Edmonds, C. G. *J. Chromatogr.* **1991**, *559*, 197.
24. Smith, R. D.; Barinaga, C. J.; Udseth, H. R. *Anal. Chem.* **1988**, *60*, 1948.
25. Ogorzalek Loo, R. R.; Udseth, H. R.; Smith, R. D. *J. Am. Soc. Mass Spectrom.* **1992**, *3*, 695.
26. Ogorzalek Loo, R. R.; Loo, J. A.; Udseth, H. R.; Fulton, J. L.; Smith, R. D. *Rapid Commun. Mass Spectrom.* **1992**, *6*, 159.
27. Richards, F. M.; Wyckoff, H. W. In *The Enzymes*, Vol. 4, 3rd ed.; Boyer, P. D., Ed.; Academic: New York, 1971; p 647.
28. Richards, F. M.; Vithayathil, P. J. *J. Biol. Chem.* **1959**, *243*, 1459.
29. Schreier, A. A.; Baldwin, R. L. *Biochemistry* **1977**, *16*, 4203.
30. Chowdhury, S. K.; Katta, V.; Chait, B. T. In *Methods and Mechanisms for Producing Ions from Large Molecules*, Standing, K. G.; Eng, W., Eds.; Plenum: New York, 1991; p 201.
31. Loo, J. A.; Edmonds, C. G.; Smith, R. D.; Lacey, M. P.; Keough, T. *Biomed. Environ. Mass Spectrom.* **1990**, *19*, 286.
32. Ogorzalek Loo, R. R.; Goodlett, D. R.; Smith, R. D.; Loo, J. A. *J. Am. Chem. Soc.* **1993**, *115*, 4391.
33. Chowdhury, S. K.; Katta, V.; Beavis, R. C.; Chait, B. T. *J. Am. Soc. Mass Spectrom.* **1990**, *1*, 382.
34. Hearn, R. P.; Richards, F. M.; Sturtevant, J. M.; Watt, G. D. *Biochemistry*, **1971**, *10*, 806.